



2009

Stable T_2Si_n ($T=Fe,Co,Ni, 1 \leq n \leq 8$) cluster motifs

R. Robles

Virginia Commonwealth University

S. N. Khanna

Virginia Commonwealth University, snkhanna@vcu.edu

Follow this and additional works at: http://scholarscompass.vcu.edu/phys_pubs

 Part of the [Physics Commons](#)

Robles, R., Khanna, S. N. Stable T_2Si_n ($T=Fe,Co,Ni, 1 \leq n \leq 8$) cluster motifs. *The Journal of Chemical Physics* 130, 164313 (2009). Copyright © 2009 AIP Publishing LLC.

Downloaded from

http://scholarscompass.vcu.edu/phys_pubs/195

This Article is brought to you for free and open access by the Dept. of Physics at VCU Scholars Compass. It has been accepted for inclusion in Physics Publications by an authorized administrator of VCU Scholars Compass. For more information, please contact libcompass@vcu.edu.

Stable T_2Si_n ($T=Fe, Co, Ni, 1 \leq n \leq 8$) cluster motifsR. Robles and S. N. Khanna^{a)}*Department of Physics, Virginia Commonwealth University, Richmond, Virginia 23284-2000, USA*

(Received 27 February 2009; accepted 3 April 2009; published online 29 April 2009; corrected 1 May 2009)

First principles studies on the geometry, electronic structure, and magnetic properties of neutral and anionic Fe_2Si_n , Co_2Si_n , and Ni_2Si_n ($1 \leq n \leq 8$) clusters have been carried out within a gradient corrected density functional framework. It is shown that these clusters display a variety of magnetic species with varying magnetic moment and different magnetic coupling between the two transition metal atoms. While Fe_2Si_n clusters are mostly ferromagnetic with large moments, Ni_2Si_n clusters are mostly nonmagnetic. Our studies of the variation of the binding energy upon addition of successive Si atoms and the gap between the highest occupied molecular orbital and the lowest unoccupied molecular orbital indicate that many of the motifs are quite stable and could be suitable as building blocks for generating magnetic cluster assembled materials. The studies also reveal motifs that could be used in molecular electronic devices to generate spin polarized currents or large magnetoresistance. © 2009 American Institute of Physics. [DOI: 10.1063/1.3123808]

I. INTRODUCTION

One of the major objectives of the current research on small clusters is to identify cluster motifs that can serve as the building blocks of nanoscale materials.¹⁻⁵ Since the properties of clusters are determined by size, composition, and the charged state, it is envisioned that by selecting the desirable building block from this pool of stable motifs, one may be able to achieve a precise control over the properties of the nanomaterials. Previous work on fullerides⁶ demonstrated the feasibility of this concept for materials assembled from alkali atoms and fullerene cages. The fullerides indeed exhibit novel behaviors including high superconducting transition temperatures. Our recent work on bulk assemblies combining As_7^{3-} and As_{11}^{3-} anion clusters with alkali and noble metal based counterions further illustrates the formation and diversity of behavior.^{5,7} Indeed, we have shown⁷ that cluster assemblies ranging from linear chains, two dimensional sheets, and three dimensional solids can be synthesized by using appropriate conditions. Spectroscopic measurements as well as theoretical calculations confirm that the assemblies built from the same polyvalent anion can exhibit band gaps ranging from 0.9 to 2.2 eV depending on the counterion. It will be ideal if similar motifs could be identified for other classes of materials that could lead to tunable characteristics. The present paper explores these avenues for silicon transition metal systems with the hope of creating magnetic silicon based semiconductors. Here we focus on motifs made of silicon with iron, cobalt, or nickel atoms.

Both carbon and silicon belong to group IV of the periodic table, however, they exhibit differing characteristics. Unlike carbon, Si prefers sp^3 bonding, favors tetrahedral coordination, and graphiticlike sheets or fullerene-like cages of silicon atoms have not been observed. The silicon cages can be stabilized by loading them with an endohedral atom⁸ and

this started a flurry of activity in making magnetic silicon cages by using transition metal endohedral atoms.⁹⁻¹⁸ However, it was found that there was a strong mixing between the d -states of the transition metal with the sp -states of the surrounding Si atoms. While this mixing stabilized the caged structure, the pairing of the electrons quenched the spin moments on the metal atom.^{13,17,18} In a recent paper,¹⁹ we proposed that the quenching of the spin moment could be avoided by introducing multiple transition metal atoms and examined this for the case of T_2Si_n ($T=Cr, Mn, 1 \leq n \leq 8$) containing two Cr or Mn atoms. In particular, we had identified Mn_2Si_4 to be a potential motif for magnetic semiconductor assemblies.

In this work, we extend our earlier investigations to T_2Si_n ($1 \leq n \leq 8$) clusters containing Fe, Co, and Ni as T atoms. The basic objective is to identify motifs that are stable and possibly display magnetic moments and diverse magnetic couplings. Recent investigations have indicated that such motifs could also lead to interesting transport properties in molecular electronics.²⁰ The studies demonstrate, for example, the presence of highly spin polarized transmissions in transition metal encapsulated silicon cages (TSi_{12}) containing Fe atoms.

In Sec. II we describe the theoretical approach while Sec. III presents the results and a discussion of results. Section IV is dedicated to final conclusions.

II. THEORETICAL APPROACH

The theoretical studies were carried out within a density functional framework using an all electron linear combination of atomic orbitals molecular orbital approach. The exchange correlation contributions were incorporated using generalized gradient functionals proposed by Perdew *et al.*²¹ In the scheme used by us, the atomic wave functions are built from Gaussian bases. The ground states were determined by calculating the forces at the atomic sites and the

^{a)}Electronic mail: snkhanna@vcu.edu.

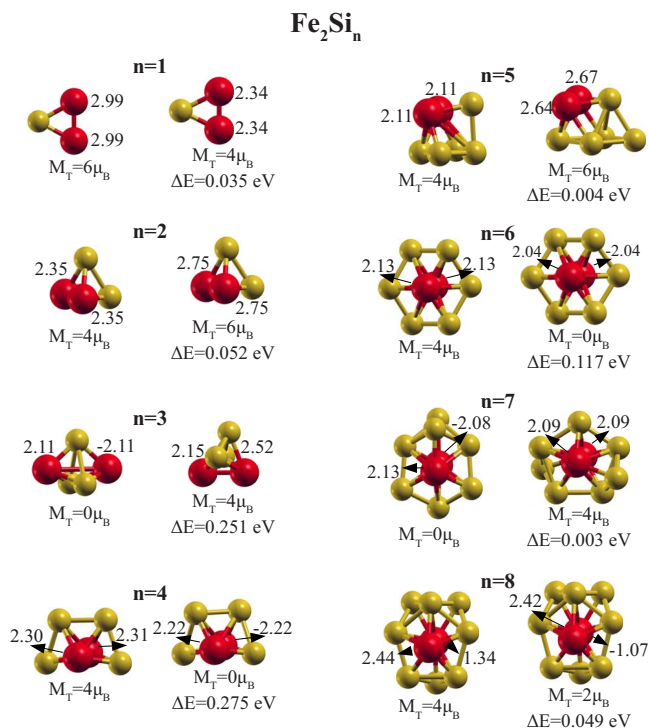


FIG. 1. (Color online) Equilibrium geometries, total spin moment M_T , and local spin moment at the transition metal atoms (in μ_B , marked beside each site) of the neutral Fe_2Si_n clusters for the ground state and the lowest higher energy isomer of the cluster. For the isomer the increment of energy with respect to the ground state, ΔE , is also listed. Dark gray (red [light gray (yellow)]) balls represent iron (silicon) atoms.

atoms were allowed to relax along the path of steepest descent till the forces dropped below a threshold value of 0.05 eV/Å. No external symmetry constrictions were imposed. Since the calculations are carried out at 0 K, the cluster can get trapped in local minima of the potential energy surface. Consequently, several magnetic and geometrical starting configurations were used to search for the ground state and higher energy isomers. For small clusters, considered in this work, such an approach provides a fairly extensive search of the potential energy surface. For larger clusters, however, global optimization techniques²² are needed to ascertain the ground state structure.

The actual calculations were based on the Naval Research Laboratory Molecular Orbital Library (NRLMOL) set of codes developed by Pederson and co-workers.^{23–25} We used a 6s, 5p, and 3d basis set for the Si atoms and 7s, 5p, and 4d bases for Fe, Co, and Ni atoms. In all cases the basis sets were complemented with a diffuse orbital. For the calculation of the local magnetic moments we have integrated the spin charge density in a sphere of 1.17 Å for Si, 1.16 Å for Fe and Co, and 1.15 Å for Ni. The total magnetic moments are unambiguously defined as the difference between the numbers of spin up and spin down electrons occupying the molecular orbitals of the cluster.

The theoretical investigations were carried out on neutral as well as anionic $T_2\text{Si}_n$ ($T=\text{Fe, Co, Ni}$, $1 \leq n \leq 8$) clusters. The results on anionic clusters are primarily targeted toward future experiments on negative ion photodetachment spectroscopy.^{14,26} These experiments involve transitions from the ground state of the anions to the neutral species and are

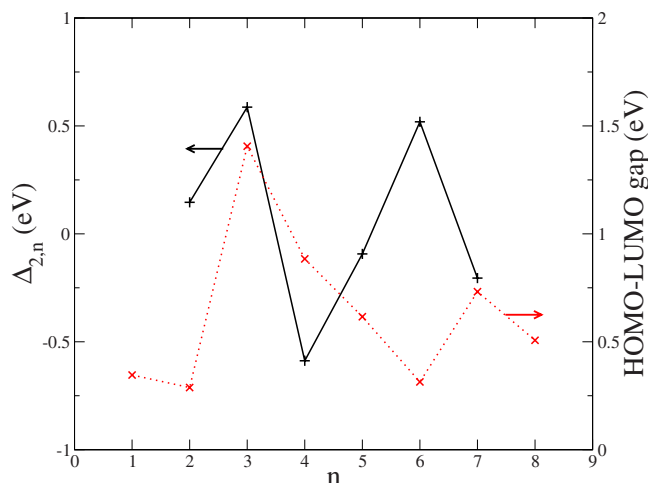


FIG. 2. (Color online) $\Delta_{2,n}$ (as defined in the text) and HOMO-LUMO gaps for neutral Fe_2Si_n clusters.

one of the only known experimental methods to provide information on the spin multiplicity and the ground state geometry, in combination with theory. Consequently, we studied the vertical detachment energies (VDEs) from the anion with multiplicity M to neutral species with multiplicity $M \pm 1$. As there are no existing measurements on the present systems, the theoretical predictions should serve as a stimulus to future experiments.

III. RESULTS AND DISCUSSION OF RESULTS

We begin with our findings on Fe_2Si_n clusters. Figure 1 shows the most stable geometries that we have found, the total spin moment M_T , and the local spin moment at the transition metal atoms of the neutral iron-silicon clusters for

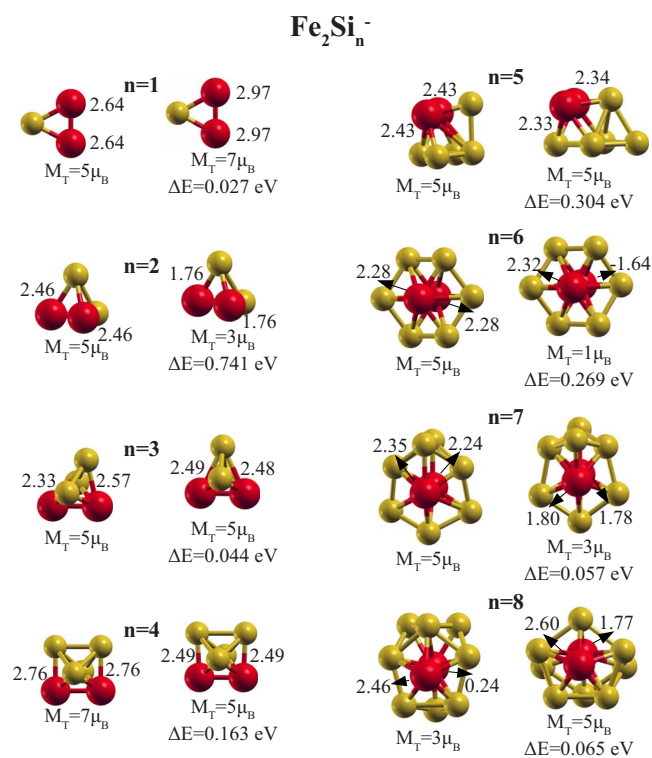


FIG. 3. (Color online) As in Fig. 1 but for Fe_2Si_n^- anions.

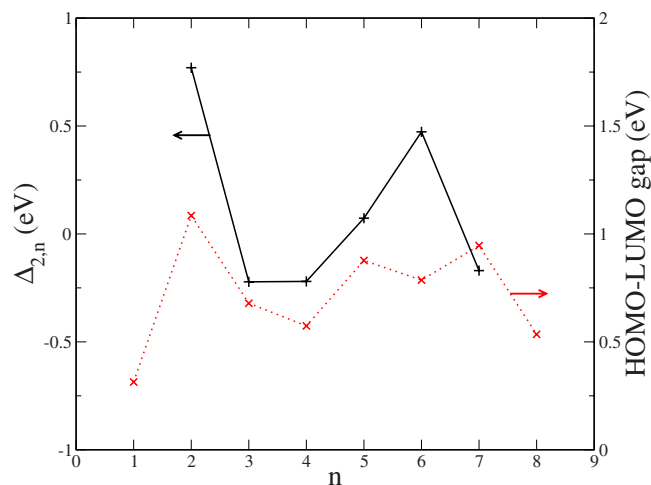


FIG. 4. (Color online) $\Delta_{2,n}$ (as defined in the text) and HOMO-LUMO gaps for $Fe_2Si_n^-$ anions.

the ground state and the lowest higher energy isomer of the cluster. Also listed are the total spin moment M_T , local moment at the individual sites, and the relative energy, ΔE , of the higher energy isomer with respect to the ground state. The Si atoms surround the Fe sites to form compact structures with Fe-Fe bonds either intact or stretched. The local coordination of the Fe and Si atoms increases from two to six as the size increases. The ground state of a free Fe_2 molecule has a spin magnetic moment of $6\mu_B$ resulting from a pair of aligned local moments of $2.82\mu_B$.²⁷ The addition of Si reduces the moment and, in many cases, modifies the magnetic coupling. For example, Fe_2Si_3 is the smallest cluster to have antiferromagnetically coupled Fe sites, with a ferromagnetic state only 0.25 eV higher in energy. A similar situation occurs for Fe_2Si_7 , where the antiferromagnetic (AF) and ferromagnetic states are virtually degenerate in energy. In all other cases, the ground state is ferromagnetic with a moment of $6.0\mu_B$ for Fe_2Si and $4.0\mu_B$ for the rest of the clusters. As mentioned in Sec. I, one of the important quantities is the stability of the species. This not only governs their intensity in cluster beams, but also facilitate their use in molecular electronics or in forming cluster assemblies. Here, we use two markers of stability that address the energetic stability as well as the chemical one. The former is examined by comparing the gain in energy in forming the cluster from the

TABLE I. AEA, VDEs from the anion with multiplicity M to neutral species with multiplicity $M \pm 1$ ($VDE^{M \pm 1}$), and VIPs for Fe_2Si_n clusters. All energies are given in eV.

Cluster	AEA	VDE^{M+1}	VDE^{M-1}	VIP
Fe_2Si_1	1.383	1.423	1.467	6.805
Fe_2Si_2	1.809	1.963	1.826	6.871
Fe_2Si_3	1.611	2.237	1.975	7.060
Fe_2Si_4	2.222	2.724	2.440	7.153
Fe_2Si_5	2.464	2.616	2.616	7.219
Fe_2Si_6	2.541	3.184	2.649	6.736
Fe_2Si_7	2.663	3.042	2.991	7.158
Fe_2Si_8	2.750	2.828	3.192	7.043

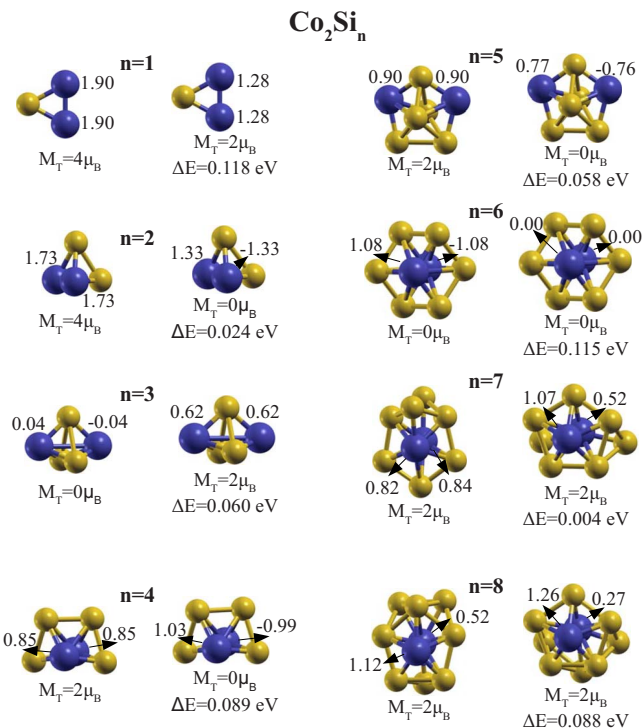


FIG. 5. (Color online) Same as in Fig. 1 but for Co_2Si_n neutrals. In this case Co atoms are represented by dark gray (blue) balls, while light gray (yellow) ones represent silicon atoms.

preceding size and the gain in energy in growing to the next size. To quantify this, we use the parameter $\Delta_{2,n}$ defined as

$$\Delta_{2,n} = -[2E(Fe_2Si_n) - E(Fe_2Si_{n+1}) - E(Fe_2Si_{n-1})].$$

With this definition, large positive values of $\Delta_{2,n}$ are indicative of enhanced stability as they correspond to a larger gain in energy in forming from the preceding size and lower gain in energy in growing to the next size. Figure 2 shows the calculated $\Delta_{2,n}$ as a function of cluster size. Note that $\Delta_{2,n}$ exhibits peaks at $n=3$ and 6. For the chemical stability, we examine it by calculating the difference between the highest occupied molecular orbital (HOMO) and the lowest unoccupied molecular orbital (LUMO).²⁸ Large values of HOMO-

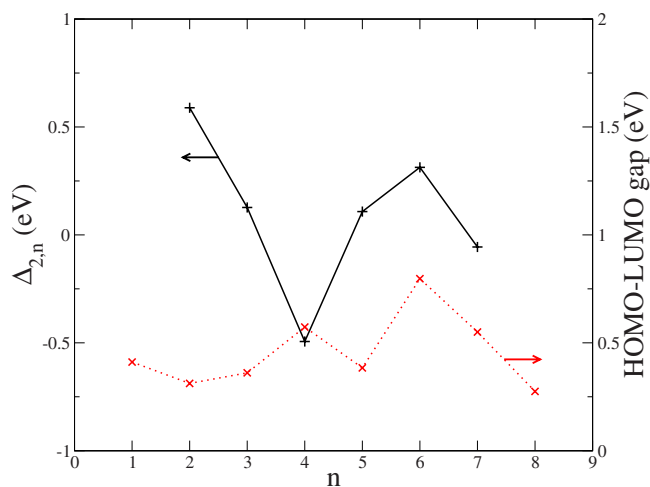
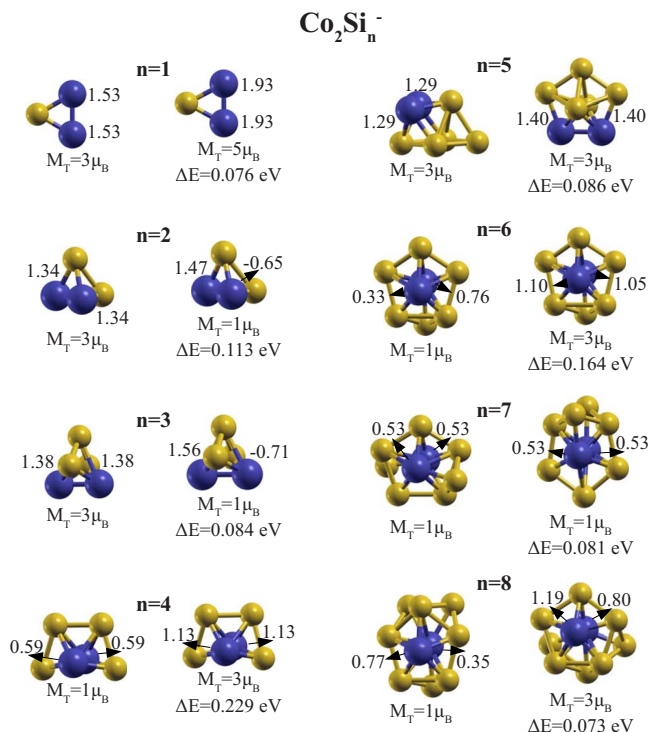
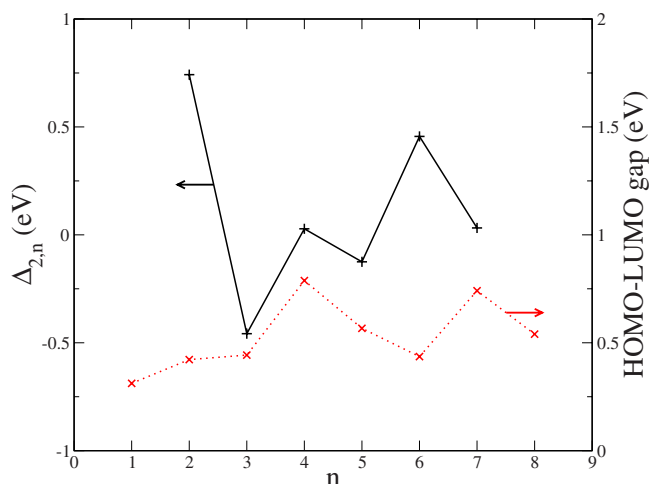


FIG. 6. (Color online) $\Delta_{2,n}$ (as defined in the text) and HOMO-LUMO gaps for neutral Co_2Si_n clusters.

FIG. 7. (Color online) As in Fig. 5 but for Co_2Si_n^- anions.

LUMO gaps are indicative of chemical inertness as the cluster wants to neither donate charge nor gain charge. The calculated HOMO-LUMO gaps are also shown on Fig. 2. Note that Fe_2Si_3 has a large HOMO-LUMO gap of 1.41 eV, while Fe_2Si_6 has a lower gap of 0.31 eV. This is interesting as these units could be used in molecular electronic devices with differing possibilities. Fe_2Si_3 with AF ground state and a close ferromagnetic state could provide a system where the current could be altered by applying a magnetic field that changes the coupling. On the other hand, Fe_2Si_6 would lead to a polarized current, as shown in recent studies on MnSi_{12} .²⁰

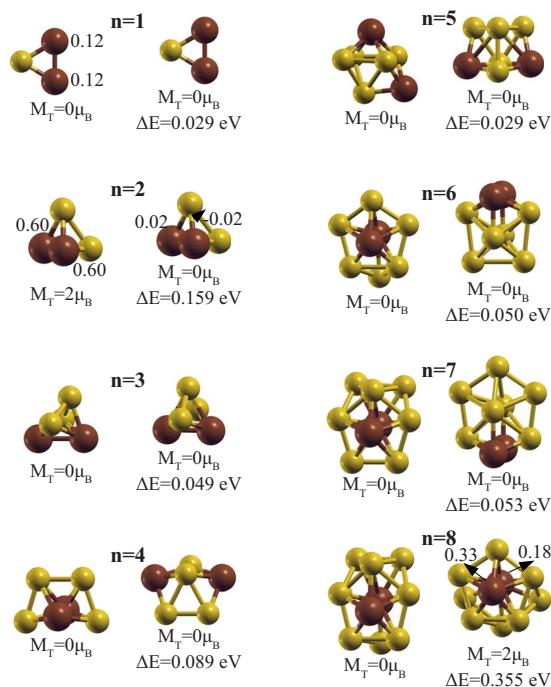
In molecular systems, the coupling between the atoms can be altered by changing the charged state as described in our previous paper²⁹ on Cr_2 and Mn_2 . Keeping this in mind,

FIG. 8. (Color online) $\Delta_{2,n}$ (as defined in the text) and HOMO-LUMO gaps for Co_2Si_n^- anions.TABLE II. Same as in Table I but for Co_2Si_n clusters. All energies are given in eV.

Cluster	AEA	VDE ^{M+1}	VDE ^{M-1}	VIP
Co_2Si_1	1.341	1.385	1.491	6.971
Co_2Si_2	1.519	1.601	1.620	6.938
Co_2Si_3	1.544	2.166	2.063	6.272
Co_2Si_4	2.154	2.275	2.537	7.080
Co_2Si_5	2.242	2.479	2.561	6.809
Co_2Si_6	2.563	2.799	3.105	6.594
Co_2Si_7	2.741	2.941	2.886	7.052
Co_2Si_8	2.829	2.863	3.194	6.958

and in order to make contact with experimental studies using negative ion photodetachment spectroscopy, we undertook a theoretical study of anionic Fe_2Si_n^- clusters. Figure 3 shows the geometry of the ground state and the first higher energy structure. Also shown are the total spin magnetic moment and the local spin moment at the various sites. Like neutral, the anions also present compact structures. The most striking difference is the change in the magnetic ordering. All the anions have ferromagnetically ordered spin moments located at the Fe site. More importantly, except for Fe_2Si_4^- and Fe_2Si_8^- , all the clusters have a spin magnetic moment of $5.0\mu_B$, showing that the addition of Si beyond Fe_2Si_4^- does not reduce the total magnetic moment. A study of $\Delta_{2,n}$, shown in Fig. 4, reveals that Fe_2Si_2^- and Fe_2Si_6^- are more stable than other sizes. These clusters also have substantial HOMO-LUMO gaps (Fig. 4), indicating their chemical as well as energetic stability. To make contact with future experiments using negative ion photodetachment spectra, we

Ni_2Si_n

FIG. 9. (Color online) Same as in Fig. 1 but for Ni_2Si_n neutrals. In this case Ni atoms are represented by dark gray (brown) balls, while light gray (yellow) ones represent silicon atoms. The local spin moments are only shown when different from $0.00\mu_B$.

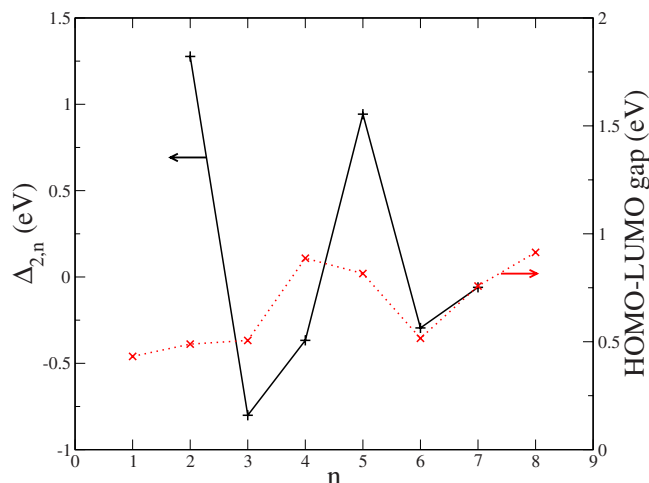


FIG. 10. (Color online) $\Delta_{2,n}$ (as defined in the text) and HOMO-LUMO gaps for Ni_2Si_n neutrals.

also calculated the adiabatic electron affinity (AEA) and the VDEs from the anion with multiplicity M to neutral species with multiplicity $M \pm 1$. The AEA is the energy difference between the ground states of the anion and the neutral clusters. These are given in Table I along with the vertical ionization potentials (VIPs) of the neutral species. What is quite intriguing is that the AEA increases monotonically as Si atoms are added. The VIP, on the other hand, shows a minimum at $Fe_2Si_6^-$, consistent with a low HOMO-LUMO gap.

We next consider the case of Co_2Si_n clusters. Figure 5 shows the equilibrium geometries, the total spin moment M_T , and the local spin moment of the neutral cobalt-silicon clusters for the ground state and the lowest higher energy isomer

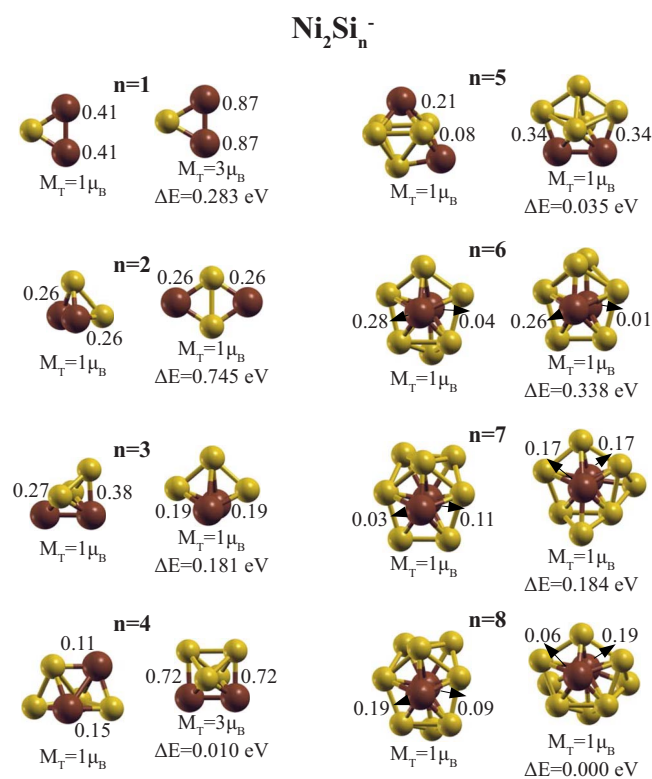


FIG. 11. (Color online) As in Fig. 9 but for $Ni_2Si_n^-$ anions.

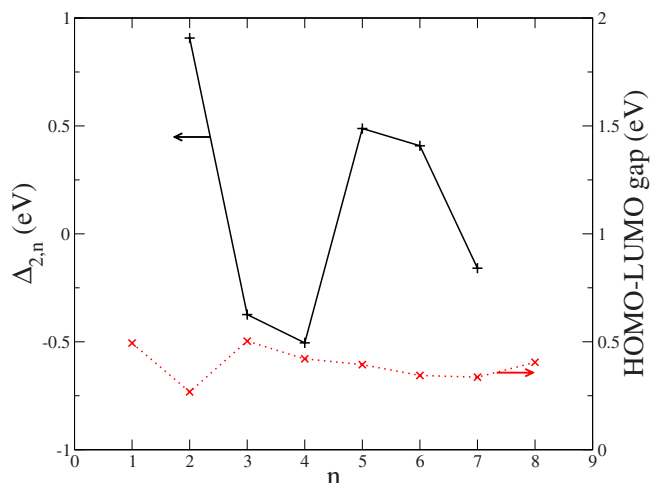


FIG. 12. (Color online) $\Delta_{2,n}$ (as defined in the text) and HOMO-LUMO gaps for $Ni_2Si_n^-$ anions.

of the cluster. In general, the magnetic moments in cobalt systems are smaller than those in the iron based clusters. The clusters containing one, two, four, five, seven, and eight Si atoms have ferromagnetic ground states, while those having three and six Si atoms have antiferromagnetically coupled moments. In particular, Co_2Si_6 has a close lying nonmagnetic (NM) state. The corresponding $\Delta_{2,n}$ and HOMO-LUMO gap are shown in Fig. 6. Co_2Si_2 and Co_2Si_6 are the more stable and Co_2Si_6 also has the highest HOMO-LUMO gap. Upon adding an electron, the cobalt based clusters do exhibit interesting progressions. As Fig. 7 shows, the clusters having one, two, three, and five Si atoms have a net spin moment of $3\mu_B$, while the remaining clusters have only one unpaired electron. The calculated $\Delta_{2,n}$ and HOMO-LUMO are shown in Fig. 8 and indicate $Co_2Si_2^-$ and $Co_2Si_6^-$ as the stable species. Finally Table II gives the AEA affinities, the VDE from the anion to the neutral, and the VIP of the neutral clusters. It is quite intriguing that the AEA shows the same progressions as in the iron based clusters.

Our final systems are the Ni_2Si_n clusters. An individual Ni atom has a spin multiplicity of 3 and we wanted to examine if the spin moment could survive under bonding with Si atoms. Figure 9 shows the ground state geometries, the total spin moment M_T , and the local spin moment of the neutral nickel-silicon clusters and the lowest higher energy isomer of the cluster. Except for Ni_2Si_1 and Ni_2Si_2 , the spin moment is quenched in all the clusters. This is consistent

TABLE III. Same as in Table I but for Ni_2Si_n clusters. All energies are given in eV.

Cluster	AEA	VDE $^{M+1}$	VDE $^{M-1}$	VIP
Ni_2Si_1	1.459	1.573	1.523	7.219
Ni_2Si_2	1.518	1.586	1.804	7.072
Ni_2Si_3	1.947	2.225	2.209	6.924
Ni_2Si_4	1.948	2.426	2.256	7.293
Ni_2Si_5	2.088	2.693	2.171	7.170
Ni_2Si_6	2.682	3.066	2.727	7.233
Ni_2Si_7	2.574	3.134	2.645	7.217
Ni_2Si_8	2.564	3.115	2.769	7.105

TABLE IV. Total spin moment (in μ_B) for T_2Si_n ($T=Cr, Mn, Fe, Co, Ni$, $1 \leq n \leq 8$) clusters. When different from ferromagnetic, the spin coupling between transition metal atoms is also indicated as AF or NM. Results for Cr_2Si_n and Mn_2Si_n are taken from Ref. 19.

n	Cr_2Si_n	Mn_2Si_n	Fe_2Si_n	Co_2Si_n	Ni_2Si_n
1	0 (AF)	8	6	4	0
2	0 (AF)	8	4	4	2
3	6	6	0 (AF)	0 (AF)	0 (NM)
4	0 (AF)	0 (AF)	4	2	0 (NM)
5	0 (AF)	8	4	2	0 (NM)
6	0 (NM)	4	4	0 (AF)	0 (NM)
7	0 (NM)	4	0 (AF)	2	0 (NM)
8	0 (NM)	0 (AF)	4	2	0 (NM)

with our previous study on supported nickel clusters,³⁰ where it was shown that the $sp-d$ hybridization easily suppresses the spin magnetic moments in nickel. Studies of $\Delta_{2,n}$ and HOMO-LUMO gap shown in Fig. 10 indicate that Ni_2Si_2 and Ni_2Si_5 are particularly stable. The quenching of the moment also results in all the anionic clusters having only one unpaired electron. This can be seen in Fig. 11 that shows the geometry and properties of the anionic species. The corresponding $\Delta_{2,n}$ and HOMO-LUMO gap are shown in Fig. 12 and $Ni_2Si_2^-$ and $Ni_2Si_5^-$ appear to have larger $\Delta_{2,n}$ than the other sizes. Finally, Table III gives the calculated AEA, the VDE from anion to the neutral species, and the VIP of all the clusters.

A key objective of the present studies has been to provide comprehensive data on T_2Si_n clusters with regard to their magnetic moments and magnetic coupling. To this end, we combine our present findings along with those on Cr_2Si_n and Mn_2Si_n (Ref. 19) to provide such information on all the species. This is shown in Table IV that combines all our findings on the total spin moment and spin coupling between transition metal atoms in T_2Si_n ($T=Cr, Mn, Fe, Co, Ni$, $1 \leq n \leq 8$) clusters. Depending on the size and the element, one finds AF, ferromagnetic, and NM behaviors. While Cr based clusters are predominantly antiferromagnetic, Mn, Fe, and Co based ones are mainly ferromagnetic, and while Ni based clusters are mostly NM. This, along with the information on stability and HOMO-LUMO gap, forms a strong base of knowledge not only for exploring cluster assemblies through direct deposition of clusters, but also in the area of molecular electronics. As mentioned before, Kong and Chelikowski²⁰ recently examined the electrical transport through $T@Si_{12}$ species and found a highly spin polarized transmission for Fe and Mn. The systems with a pair of transition metal atoms in Table IV not only can provide such polarized transmissions, but the progression in coupling through charging or application of fields may allow motifs with exceptional magnetoresistance. Exploration of these magnetoelectronic effects will form the basis of our future work.

IV. CONCLUSIONS

The main objective of the present work has been to provide a comprehensive base of knowledge on the stability and

the magnetic characteristics of the neutral and anionic T_2Si_n clusters containing late transition elements. The clusters with AF ground states with close ferromagnetic states would be ideal for probing magnetoresistive features at the nanosize, while the ferromagnetic species may allow spin polarized transmissions in molecular electronics. The clusters with higher $\Delta_{2,n}$ and larger HOMO-LUMO gap have better potential to maintain their identity in cluster assemblies. Finally, we hope that the information on transition energies of anionic species will stimulate experimental interest in these systems that display such a rich variety of behavior.

ACKNOWLEDGMENTS

We gratefully acknowledge support from the U.S. Department of the Army through a MURI Grant No. W911NF-06-1-0280.

- A. W. Castleman, Jr. and S. N. Khanna, *J. Phys. Chem. C* **113**, 2664 (2009).
- P. Jena, S. N. Khanna, and B. K. Rao, in *Cluster Assembled Materials*, edited by K. Sattler (Trans Tech., Zurich, 1996), Vol. 232, p. 1.
- A. Perez, P. Melinon, V. Dupuis, P. Jensen, B. Prevel, J. Tuaille, L. Bardotti, C. Martet, M. Treilleux, M. Broyer, M. Pellarin, J. L. Vaille, B. Palpant, and J. Lerme, *J. Phys. D: Appl. Phys.* **30**, 709 (1997).
- J. H. Weaver and D. M. Poirier, *Solid State Physics* (Academic, Boston, 1994), Vol. 48, p. 1.
- A. W. Castleman, Jr., S. N. Khanna, A. Sen, A. C. Reber, M. Qian, K. M. Davis, S. J. Peppernick, A. Ugrinov, and M. D. Merritt, *Nano Lett.* **7**, 2734 (2007).
- R. C. Haddon, *Acc. Chem. Res.* **25**, 127 (1992).
- M. Qian, personal communication (10 February 2009).
- K. Jackson and B. Nellerhoe, *Chem. Phys. Lett.* **254**, 249 (1996).
- V. Kumar and Y. Kawazoe, *Phys. Rev. Lett.* **87**, 045503 (2001).
- J.-G. Han and Y.-Y. Shi, *Chem. Phys.* **266**, 33 (2001).
- H. Hiura, T. Miyazaki, and T. Kanayama, *Phys. Rev. Lett.* **86**, 1733 (2001).
- T. Miyazaki, H. Hiura, and T. Kanayama, *Phys. Rev. B* **66**, 121403(R) (2002).
- S. N. Khanna, B. K. Rao, and P. Jena, *Phys. Rev. Lett.* **89**, 016803 (2002).
- W. Zheng, J. M. Nilles, D. Radisic, and K. H. Bowen, Jr., *J. Chem. Phys.* **122**, 071101 (2005).
- C. Xiao, F. Hagelberg, and W. A. Lester, *Phys. Rev. B* **66**, 075425 (2002).
- P. Sen and L. Mitas, *Phys. Rev. B* **68**, 155404 (2003).
- J. U. Reveles and S. N. Khanna, *Phys. Rev. B* **72**, 165413 (2005).
- J. U. Reveles and S. N. Khanna, *Phys. Rev. B* **74**, 035435 (2006).
- R. Robles, S. N. Khanna, and A. W. Castleman, Jr., *Phys. Rev. B* **77**, 235441 (2008).
- L. Kong and J. R. Chelikowsky, *Phys. Rev. B* **77**, 073401 (2008).
- J. P. Perdew, K. Burke, and M. Ernzerhof, *Phys. Rev. Lett.* **77**, 3865 (1996).
- K.-M. Ho, A. A. Shvartsburg, B. Pan, Z.-Y. Lu, C.-Z. Wang, J. G. Wacker, J. L. Fye, and M. F. Jarrold, *Nature (London)* **392**, 582 (1998).
- M. R. Pederson and K. A. Jackson, *Phys. Rev. B* **41**, 7453 (1990).
- K. Jackson and M. R. Pederson, *Phys. Rev. B* **42**, 3276 (1990).
- D. Porezag and M. R. Pederson, *Phys. Rev. A* **60**, 2840 (1999).
- U. Gupta, J. U. Reveles, J. J. Melko, S. N. Khanna, and A. W. Castleman, Jr., *Chem. Phys. Lett.* **467**, 223 (2009).
- Let us remember that the local magnetic moment is obtained by integrating the spin density in a sphere around the atom. Therefore, the sum of the local magnetic moments do not necessarily add to the total magnetic moment.
- A. Reber, S. Khanna, P. Roach, W. Woodward, and A. W. Castleman, Jr., *J. Am. Chem. Soc.* **129**, 16098 (2007).
- N. Desmarais, F. A. Reuse, and S. N. Khanna, *J. Chem. Phys.* **112**, 5576 (2000).
- R. Robles, R. C. Longo, A. Vega, and L. J. Gallego, *Phys. Rev. B* **62**, 11104 (2000).